

BUNCH LENGTHENING AND MICROWAVE INSTABILITY

F.J. Sacherer  
CERN, Geneva, Switzerland

Introduction and Summary

A single-bunch instability that leads to blow-up of bunch area and microwave signals (100 MHz to 3 GHz) has been observed in the PS<sup>1)</sup> and the ISR<sup>2)</sup>. A similar instability may cause bunch lengthening in electron storage rings. Attempts to explain this as a high-frequency coasting-beam instability require e-folding rates faster than a synchrotron period, and wavelengths shorter than a bunch length. In this case, the usual Keil-Schnell coasting-beam criterion<sup>3)</sup> is used, but with local values of bunch current and momentum spread, as suggested by Bousard<sup>4)</sup>. This yields  $|Z/n| \approx 13 \Omega$  for the ISR, and values about five to ten times larger for the PS. The restrictions mentioned above, however, are not fulfilled near threshold, or for frequencies as low as 100 MHz.

A direct approach, without coasting-beam approximations, is presented in this paper. The basic idea is that the usual bunched-beam modes<sup>4)</sup>, dipole, quadrupole, sextupole, etc., become unstable at intensities sufficiently high for their coherent frequencies to cross, as indicated in Fig. 1. If  $Z(\omega)$  is known, the frequency shifts can be computed, and surprisingly, one finds thresholds near the coasting beam values, but with fewer assumptions.

The lowest thresholds occur for wakefields that decay in about a bunch length. In general, lowering Q-values does not help, since the threshold depends on the area under the resonance curve. For very rapidly decaying wakes, the bunch is stable, in agreement with a conjecture of Hereward<sup>5)</sup>. Only one wavelength along the bunch is sufficient for instability.

The main results are presented here (Part 1), while the derivations are given elsewhere<sup>6)</sup> (Part 2). For other approaches, see references 7 to 10.

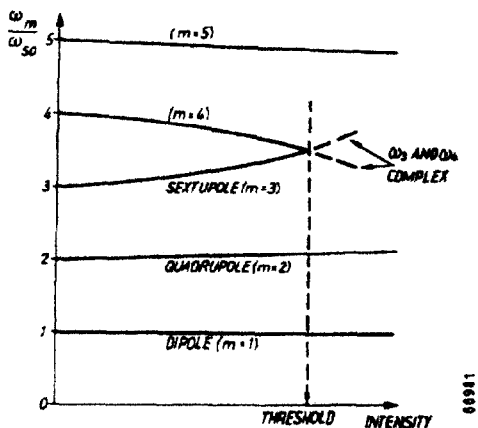


Fig. 1 Coherent frequencies  $\omega_m$  versus intensity

Modes of Oscillation

For low intensities, a bunch can oscillate in the usual dipole, quadrupole and higher modes (Fig. 2) with frequencies near harmonics of the synchrotron frequency,  $\omega_m = m\omega_{S0}$ . The oscillating part of the line density  $\lambda_m(t)$  is approximately sinusoidal, and a little thought

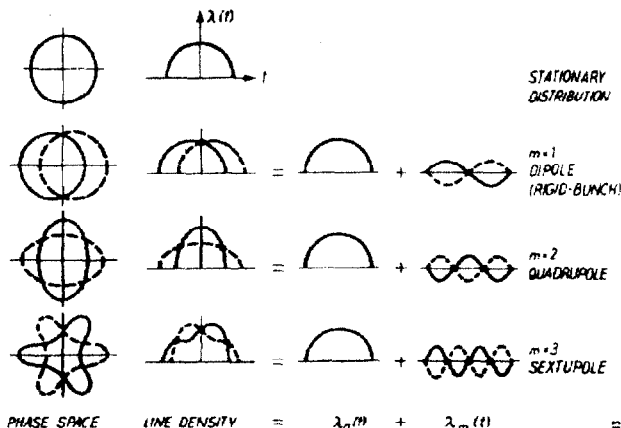


Fig. 2 Low-intensity modes of oscillation

shows it to be a standing wave with fixed nodes, so there is no instability if the wakefield decays before the next bunch arrives<sup>\*)</sup>. However, at sufficiently high intensities for two coherent frequencies to merge as indicated in Fig. 1, the two standing waves add to give travelling waves, one moving forward and one backward along the bunch, one of which is stable and the other unstable. This is the connection with the coasting-beam travelling-wave modes.

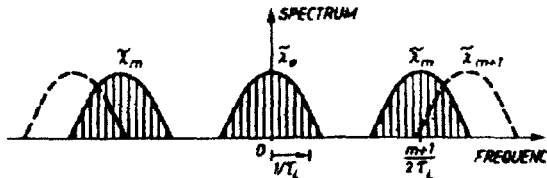


Fig. 3 Envelope of frequency spectra for the stationary distribution and for modes  $m$  and  $m+1$

The spectra for the low intensity modes are shown in Fig. 3. Mode  $m$  is peaked near the frequency  $(m+1)/2T_L$  of the sine wave  $\lambda_m(t)$ , and extends  $\pm 1/T_L$  Hz corresponding to the bunch length  $T_L$  sec. For example, mode  $m = 5$  for a 1 nsec bunch is centred at 3 GHz, and lies mostly above the pipe cut-off.

The actual spectrum is a line spectrum within the envelopes of Fig. 3. For one bunch, the frequencies

$$f_p = pf_0 + mf_s, \quad -\infty < p < \infty \quad (1)$$

occur, where  $f_s$  is the synchrotron frequency and  $f_0$  is the revolution frequency in Hz. For  $M$  equally spaced bunches, only every  $M^{\text{th}}$  line occurs,

$$f_p = (n + pM)f_0 + mf_s, \quad -\infty < p < \infty \quad (2)$$

\*) A longitudinal chromaticity due to the dependence of the synchrotron frequency on momentum deviation would lead to a head-tail instability analogous to the transverse case, but this effect has been estimated to be very small<sup>1)</sup>.

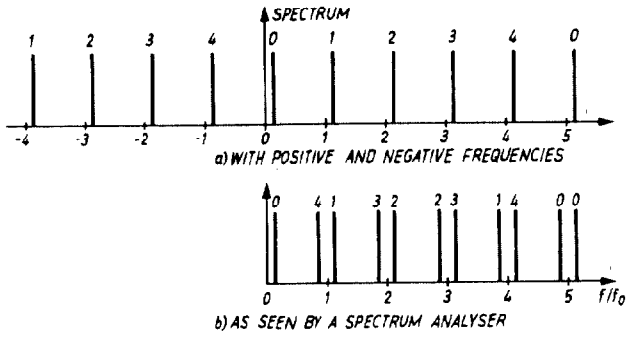


Fig. 4 Spectrum lines for coupled-bunch modes

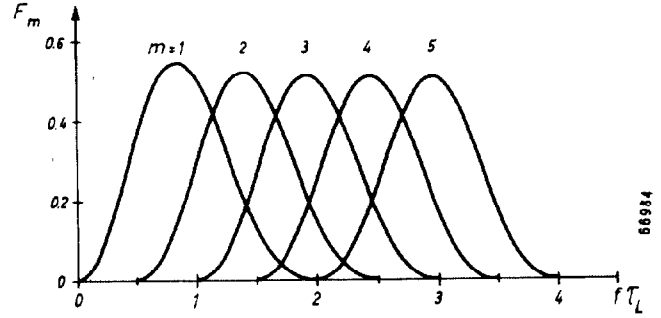


Fig. 5 Form factor

where  $n$  is the usual coupled-bunch mode number, running from 0 to  $M-1$ . The coupled-bunch modes for 5 bunches are shown in Fig. 4. Note that the negative frequency components are seen as lower sidebands by a spectrum analyser.

#### Coherent Frequencies

The coherent frequencies are solutions of the determinant

$$|\omega - m\omega_s - M_{mk}| = 0, \quad (3)$$

where the matrix element  $M_{mk}$  gives the effect of mode  $k$  on mode  $m$ . It involves the overlap of the spectral density,

$$h_{mk}(p) = \tilde{\lambda}_m^*(p) \tilde{\lambda}_k(p) \quad (4)$$

with the coupling impedance  $Z(p)/p$ . In general,

$$M_{mk} = j \frac{m\omega_s}{m+1} \frac{I_0}{3B_0^2 h V_T \cos \phi_s} \frac{\sum_p \frac{Z(p)}{p} h_{mk}(p)}{\sum_p h_{mm}(p)} \quad (5)$$

where the summations are over the mode spectra (1) or (2). Here  $\omega_s$  is the single-particle synchrotron frequency, or incoherent frequency in radians/second;  $\omega_{s0}$  is the zero-intensity synchrotron frequency;  $V_T$  is the peak RF voltage  $V_0$ , plus the space-charge or inductive-wall contribution  $V_T = (\omega_s/\omega_{s0})^2 V_0$ ;  $h$  is the RF harmonic number;  $I_0$  is the current in one bunch;  $B_0$  is the bunching factor for one bunch, bunch length  $\tau_L$ /revolution period  $T$ ;  $\phi_s$  is the synchronous phase (equal to zero for a stationary bucket), with the convention that  $\cos \phi_s$  is positive below transition and negative above. The usual convention is used for  $Z(\omega)$ , namely inductive impedance  $j\omega L$  has positive reactance.

#### Low Intensities

The diagonal elements of (3) give the usual low intensity results,

$$\omega_m = m\omega_s + M_{mm}. \quad (6)$$

Above transition, the coherent frequency  $\omega_m$  is shifted up by inductance and down by capacitance, with the opposite below transition. Figure 1 thus corresponds to the situation above transition with a resonator between modes  $m=3$  and 4, so that mostly inductance contributes to mode 3 and capacitance to mode 4.

For constant  $Z(p)/p$ , such as inductive-wall or space-charge, the summations drop out of (5), and (6) reduces to the known result<sup>4)</sup>.

Resistance contributes an imaginary frequency shift, and may cause instability depending on the sign of  $p$ . Above transition, upper sidebands are unstable and lower sidebands are stable, with the opposite below transition.

For a single bunch, or two bunches, upper and lower sidebands belong to the same coupled-bunch mode, and therefore tend to cancel unless the impedance is very narrow-band such as the RF cavity. Trouble is avoided in this case by tuning the cavity to overlap the stable sideband (Robinson criterion). For more than two bunches, upper and lower sidebands usually belong to different coupled-bunch modes (see Fig. 4), so that a resonator will drive one mode and damp the other complementary mode. The maximum growth rate is given by  $-\text{Im} \Delta\omega_m$ , where

$$\Delta\omega_m = j \frac{m\omega_s}{m+1} \frac{I}{3B_0^2 h V_T \cos \phi_s} \frac{Z(p)}{p} F_m, \quad (7)$$

$I = MI_0$  is the current in  $M$  bunches, and the form factor

$$F_m = \frac{1}{MB_0} \frac{h_{mm}(p)}{\sum_p h_{mm}(p)}$$

is plotted in Fig. 5. This is the usual result<sup>4)</sup>, but with slightly different notation. For larger bandwidths, more than one term must be included in the summation (5), and cancellation occurs between upper and lower sidebands. The growth-rate (8) is reduced by the factor  $D$  shown in Fig. 6, where  $\alpha = 2\pi M \Delta f / f_0$  is the attenuation of the wake between bunches and  $\Delta f = f_{res}/2Q$  is the resonator bandwidth. Thus there is no instability for wakefields that decay appreciably before the next bunch arrives.

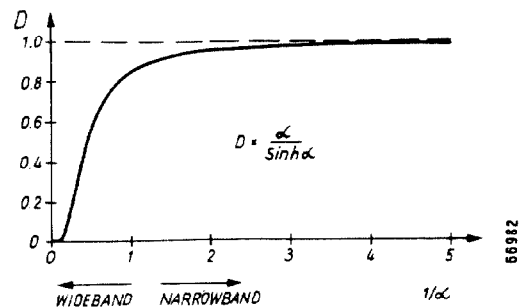


Fig. 6

#### High Intensities

For larger bandwidths, the details of the line spectra can be ignored, and the summations in (5) replaced by integrations. Then only reactance contributes to the main diagonal and even-numbered diagonals, which are symmetric; and only resistance to the odd diagonals,

which are antisymmetric. The matrix  $M$  is real, so there is no instability for zero resistance. Also, only the three central diagonals need be retained because there is little overlap or coupling for modes separated by more than one integer  $m$  (see Fig. 3).

It is convenient to introduce the dimensionless intensity parameter  $\epsilon$ ,

$$\epsilon = \frac{I_0}{2B_0^3 h V_T} \left| \frac{Z(p)}{p} \right| \cos \phi_s \quad (8)$$

where  $Z(p)/p$  will be taken to be the peak value for a resonator. The coasting-beam thresholds can be written as (Part 2)

$$\epsilon \leq 1.15 \text{ for peak current} \quad (9)$$

$$\epsilon \leq 1.73/B_{RF} \text{ for average current} \quad (10)$$

where  $B_{RF}$  = bunch length  $\tau_L$ /RF period =  $hB_0$ .

For the example shown in Fig. 1 of a resonator that couples only modes  $m = 3$  and 4, Eq. (3) reduces to

$$\begin{vmatrix} \omega - 3\omega_s - M_{33} & -M_{34} \\ M_{34} & \omega - 4\omega_s - M_{44} \end{vmatrix} = 0 \quad (11)$$

If  $\omega_3' = 3\omega_s + M_{33}$  and  $\omega_4' = 4\omega_s + M_{44}$  are the low-intensity solutions, then in general

$$\omega = \frac{1}{2} \left[ \omega_3' + \omega_4' \pm \sqrt{(\omega_4' - \omega_3' + \omega_s)^2 - 4M_{34}^2} \right] \quad (12)$$

and the threshold occurs at the crossing point where

$$|M_{34}| = \frac{1}{2} |M_{44} - M_{33} - \omega_s| \quad (13)$$

The thresholds (crossing of two crossing frequencies) have been computed for different resonator bandwidths, and are shown in Fig. 7. The solid line corresponds to a resonant frequency that lies between the maxima of two mode spectra, so that only two modes are coupled for small bandwidths; the dotted line is for a resonance that coincides with the maxima of a mode, so that at least three modes are coupled, which gives a higher threshold.

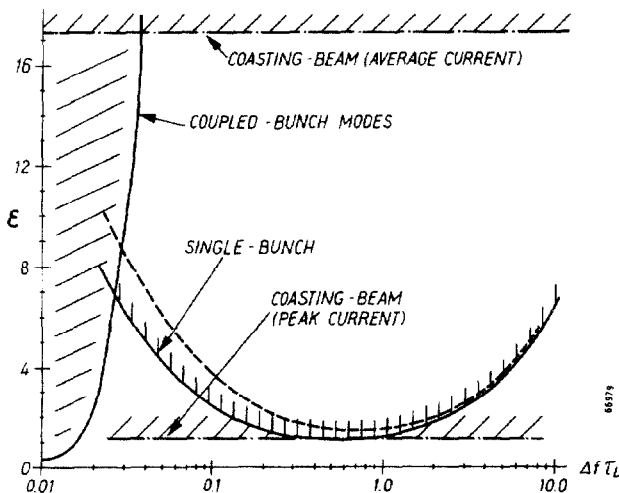


Fig. 7 Instability threshold versus bandwidth  $\Delta f$

The over-all form of the threshold curve is easily understood. For small bandwidths, only a few lines contribute to the sum (5), and the threshold is high. As the bandwidth increases, the summation grows in proportion to the area under the resonance curve, until saturation occurs when  $\Delta f$  is about as wide as the mode spectra  $1/\tau_L$ . Up to this point, a  $2 \times 2$  or  $3 \times 3$  matrix suffices. For larger bandwidths, more and more modes are coupled. The frequencies for the central modes are now pulled about equally in both directions, up or down (a metaphor due to Hereward), and so move relatively little. In the limit of large  $\Delta f$ , the bunch is stable.

For very small bandwidths (decay time  $\leq$  bunch spacing), coupled-bunch modes are unstable, and the threshold is shown in Fig. 7 for the case where every third bucket (stationary) is filled, with a bunch length  $1/10$  of the bucket length ( $hB_0 = 0.1$ ). The coasting-beam thresholds for average current (10) and peak current (9) are also shown. Finally, the factor  $m/(m+1)$  in (5) has been neglected here, so that the thresholds for the low order modes are  $(m+1)/m$  times larger than shown in Fig. 7, which is at most a factor of two. This is the price for having only one or two wavelengths along the bunch.

### Conclusion

The coasting-beam threshold for peak current is equivalent to the crossing of two coherent frequencies, which should be observable. Presumably, the bunch lengthens to remain just below this threshold. In addition, bunch lengthening due to static potential-well distortion may occur. This is caused by lower frequency impedances that overlap the stationary bunch spectrum.

### Acknowledgements

I have benefited from discussions with H.G. Hereward, and also from the hospitality of the 1976 Isabelle Summer Study. Many of the calculations for this paper were performed by Mme M. Lelaizant.

### References

- 1) D. Boussard, CERN Int. Rep. Lab. II/RF/Int. 75-2 (1975), and also these proceedings.
- 2) S. Hansen and A. Hofmann, ISR Performance Report, CERN Int. Rep. ISR-GS/RF-AH/amb (1976).
- 3) E. Keil and W. Schnell, CERN Int. Rep. CERN-TH/RF/69-48 (1969).
- 4) F. Sacherer, Proc. 5th US Particle Accelerator Conf., San Francisco, 1973, IEEE Trans. Nuclear Sci. NS-20, 825 (1973), and also F. Pedersen and F. Sacherer, these proceedings.
- 5) H.G. Hereward, Proc. 1975 Isabelle Summer Study, Brookhaven BNL 20550, p. 555.
- 6) F. Sacherer, CERN Int. Rep. CERN/PS/BR/77-4 (1977).
- 7) A. Renieri, Frascati Rep., LNF-76/11(R) (1976).
- 8) E. Messerschmid and M. Month, Nuclear Instrum. Methods 136, 1 (1976), and also these proceedings.
- 9) P. Channell and A. Sessler, Nuclear Instrum. Methods 136, 473 (1976).
- 10) A. Chao and J. Gareyte, SPEAR-197, PEP-224 (1976), and also these proceedings.
- 11) H.G. Hereward, Rutherford Lab. Rep. EPIC/MC/70 (1975).